Available online at www.sciencedirect.com

ScienceDirect

Procedia Structural Integrity 39 (2022) 128–138

Structural Integrity Procedia

www.elsevier.com/locate/procedia

7th International Conference on Crack Paths

# Influence of hydrogen on the fatigue crack growth rate of 42CrMo4 steel welds: a comparison between pre-charge and in-situ testing

A. Zafra[a], G. Álvarez[a], G. Benoit[b], G. Hénaff[b], C. Rodríguez[a], J. Belzunce[a]*

[a]*SIMUMECAMAT Research Group, University of Oviedo, Polytechnic School of Engineering of Gijón, East Building, 33203, Asturias, Spain*
[b]*Institut Pprime, UPR 3346 CNRS ENSMA Université de Poitiers, Ecole Nationale Supérieure de Mécanique et d'Aérotechnique, Téléport 2, 1 Avenue Clément Ader, BP 40109, F-86961 Futuroscope Chasseneuil, France*

**Abstract**

The effects of hydrogen on the fatigue crack growth behavior of 42CrMo4 welds, present in hydrogen buffer tanks, were studied in this paper. Two different testing methodologies were compared: hydrogen pre-charge testing and in-situ testing. A comprehensive analysis of the fracture surfaces was performed using scanning electron microscopy. In general terms, the coarse grain heat affected zone was more sensitive to hydrogen embrittlement than the base steel due to its coarser and more distorted martensitic microstructure. Noticeable differences were observed between the fatigue crack growth curves obtained with pre-charged specimens and specimens tested in a hydrogen atmosphere. This behavior, as well as the influence of certain testing variables such as the frequency or the load ratio are discussed. Nevertheless, similar modifications of the fracture micromechanisms due to hydrogen were observed in both testing methodologies. The observation of internal interface decohesion under such low hydrogen concentrations proves the synergistic action of hydrogen-enhanced localized plasticity (HELP) and hydrogen-enhanced decohesion (HEDE) damage mechanisms.



*Keywords:* Hydrogen embrittlement; fatigue crack growth; CGHAZ; pre-charge testing; in-situ testing; failure mechanims

* Corresponding author. Tel.: +34 985 182 023
*E-mail address:* belzunce@uniovi.es


10.1016/j.prostr.2022.03.081

## 1. Introduction

The increasing costs of electricity in addition to the zero $CO_2$ emission policies being implemented by occidental governments, is causing the outbreak of hydrogen-based energy sources. Apart from its clean combustion, as takes place for example in hydrogen fuel-cell vehicles, this element can also be used as an efficient energy vector. In such way, the energy surplus generated in wind and solar farms during the peak hours, can be used to generate green hydrogen that can be stored for later use. However, the main drawback of hydrogen is its very low energetic density (10 MJ/m$^3$) compared to other gaseous fuels such as methane (33 MJ/m$^3$) or propane (87 MJ/m) [1]. Therefore, in order to meet the increasing energetic demands and make hydrogen an economical alternative to traditional hydrocarbons, it is necessary the use of very high operation, distribution, and storage pressures, between 30-100 MPa [2].

It is clear then that the overall efficiency of hydrogen distribution and storage infrastructures relies upon an adequate material selection. In this sense, CrMo steels, quenched and tempered to provide sufficient yield strength levels, are considered excellent candidates due to their low cost-strength ratios [3]. However, it is well known that this family of steels is susceptible to the so-called hydrogen embrittlement (HE) phenomenon. Indeed, the interaction among hydrogen atoms, the steel microstructure, and the applied loads, has been extensively studied [4]. In general terms, hydrogen diffuses in the iron lattice driven by stress and concentration gradients and is trapped in certain microstructural defects such as dislocations and internal interfaces. Eventually, when a sufficient hydrogen concentration is attained in these sites, the operative fracture micromechanism is modified, from ductile to brittle- and the mechanical properties are significantly reduced.

It was demonstrated in previous works that hydrogen accelerates the fatigue crack growth rate in a wide range of medium-high strength steels [5–8]. Therefore, assessing the degradation of fatigue properties in martensitic CrMo steels is of primary importance because hydrogen components undergo cyclic stress from the fluctuation of internal gas pressure, in addition to external loads.

There are two basic ways that have been typically used to analyse the effects of hydrogen on the crack growth rate of CrMo steels aimed to work in hydrogen gas atmospheres [9]:

(I) In-situ testing in high pressure hydrogen gas (external hydrogen) [10–13]. This method requires the use of very expensive, unique facilities, as the specimens are exposed to high-pressure hydrogen gas while simultaneously is subjected to a specific cyclic mechanical load. In addition, optical measurements and/or a direct current potential drop (DCPD) technique may be used to the measurement of the crack extension along the tests. Its main advantage is that using this methodology, the real operation conditions may be reproduced.

(II) Testing in air after pre-charging the specimens in a gaseous hydrogen medium (internal hydrogen) [14]. This is a simple and convenient alternative that consists in pre-charging the specimens with hydrogen and then performing conventional fatigue crack growth tests in air. As hydrogen diffusion depends exponentially on temperature, the use of high temperatures greatly accelerates hydrogen pre-charging in a gaseous hydrogen atmosphere providing high hydrogen contents after relatively short charging times.

In general it is accepted that the fundamental interactions between hydrogen and the steel microstructure do not depend on the test methodology once hydrogen was dissolved into the metal [8,15]. For this reason, several studies on the effect of hydrogen on the FCGR of steels have been performed using pre-charged specimens. Although this can be considered an acceptable approach when studying the effects of hydrogen on the fatigue behaviour of austenitic steels or Ni based alloys, where room temperature (RT) diffusivity of hydrogen is very low - of the order of $10^{-15}$-$10^{-16}$ m$^2$/s - and solubility very high, this may not be the case when dealing with quenched and tempered CrMo steels. The latter usually have diffusivities in the order of $10^{-10}$-$10^{-12}$ m$^2$/s, and low hydrogen solubilities at RT. Having this in mind, the hydrogen distribution in martensitic CrMo specimens in the course of the fatigue test may be different when using internal or external hydrogen, which will eventually determine the amount of hydrogen reaching the crack tip process region each loading cycle, and therefore the extent of hydrogen embrittlement.

It is unclear then whether testing procedure could have a relevant impact in the obtained results, leading to an incorrect comparison of the results obtained with both testing methodologies. Few references exist on this particular matter. Therefore, this work aims to assess the influence of hydrogen on the fatigue crack growth behaviour of 42CrMo4 steel welds by means of hydrogen pre-charged samples and in-situ testing. A thorough comparison of the results obtained through both methodologies along with a comprehensive study of the fracture micromechanisms was carried out. The combined set of data help us in advancing the understanding of the complex interaction between hydrogen atoms, the steel microstructure, and the fatigue loads, as well as the influence of certain testing variables such as the frequency and the load ratio.

**Nomenclature**

| | |
|---|---|
| BS | base steel |
| CGHAZ | coarse grain heat affected zone |
| CT | compact tensile specimens |
| DCPD | direct current potential drop |
| ΔK | stress intensity factor range |
| f | frequency |
| FCGR, da/dN | fatigue crack growth rate |
| FCGRT | fatigue crack growth rate tests |
| HAZ | heat affected zone |
| HE | hydrogen embrittlement |
| HEDE | hydrogen enhanced decohesion |
| HELP | hydrogen enhanced localized plasticity |
| IG | intergranular |
| In-situ | test performed in a high-pressure hydrogen environment |
| MLD | martensitic lath decohesion |
| R | load ratio |
| RT | room temperature |
| SEM | scanning electron microscopy |
| wppm | weight parts per million |

## 2. Experimental methods

### *2.1. Steel and heat treatments*

A commercial 42CrMo4 (0.42%C-0.98%Cr-0.22%Mo) steel was used in the present study. 250x250x12 mm hot rolled plates were austenitized at 845ºC for 40 min, quenched in water and tempered at 700ºC for 2h (Base Steel, BS). Then, a weld bead from a carbon steel wire was deposited applying a heat input of 1.96 kJ/mm. A thorough characterization of the weld was carried out and the coarse grain heat affected zone (CGHAZ) was identified as the coarsest and hardest microstructure in the weld, and therefore the area more prone to suffer from HE [16].

In order to machine standard size compact tension (CT) specimens for an accurate characterization of the fatigue behavior, the microstructure developed in the CGHAZ was reproduced by austenitizing at 1200ºC for 20 min and quenching in oil. A coarse and hard martensitic microstructure with a prior austenitic grain size (PAGS) of 100-150 was obtained, similar to the real CGHAZ. Finally, the same tempering treatment applied to the BS (700ºC for 2h) was applied to the CGHAZ for microstructural recovery. For more details on weld characterization and the simulation process of the CGHAZ the reader is referred to [17].

Table 1 shows that the BS and CGHAZ displayed quite similar hardness (HV30) and tensile properties, being the main difference the prior austenitic grain size (PAGS) [17]. In both steels the microstructure was tempered martensite.

Table 1. Hardness, PAGS and tensile properties of the BM and the CGHAZ [17].

| Steel | HV30 | PAGS (μm) | $\sigma_{ys}$ (MPa) | $\sigma_{ut}$ (MPa) | E (%) | Z (%) |
|---|---|---|---|---|---|---|
| BM | 207 | 2 | 622 | 710 | 22.6 | 61.3 |
| CGHAZ | 230 | 4 | 600 | 750 | 23.6 | 65.5 |

*2.2. Fatigue crack growth tests*

The influence of hydrogen on the fatigue behaviour of 42CrMo4 steel welds was assessed by means of FCGRT performed (I) in air onto hydrogen pre-charged samples and (II) in a high-pressure hydrogen gas environment.

*2.2.1. Tests on hydrogen pre-charged samples*

These FCGRT were performed using CT specimens with a width of 48 mm and a thickness of 10 mm. Before hydrogen pre-charging, the specimens were fatigue pre-cracked in air at R=0.1 and 10 Hz following the ASTM E647 standard [22] up to achieving an initial crack length, $a_0$=7 mm (a/W=0.15).

The specimens were pre-charged in a high-pressure reactor at 19.5 MPa of pure gaseous hydrogen and 450ºC for 21 hours. A similar hydrogen content of around 1.2-1 wppm was introduced in both the BS and the CGHAZ under this charging conditions.

The FCGT were performed in air at RT using a servohydraulic universal MTS testing machine equipped with a load cell of 250 kN. A constant ΔP load was applied from an initial stress intensity factor range ($\Delta K_0$) between 30-40 MPa$\sqrt{m}$. In the course of the fatigue crack growth tests, the crack length was continuously monitored by means of a CTOD extensometer, allowing the representation of da/dN vs. ΔK curves. The initial and final crack lengths were measured on the fracture surface of the broken specimen, and the measured ΔK values were accordingly corrected.

Uncharged specimens were also tested at a load ratio R=0.1 and a frequency f=10 Hz. The hydrogen pre-charged specimens were tested at R=0.1 and f=1 and 0.1 Hz, as lower frequencies have been reported to be detrimental for the fatigue crack growth behaviour in presence of hydrogen [14,18].

*2.2.2. In-situ testing in hydrogen gas*

FCGRT were conducted in the Hycomat test bench developed by Pprime institute at RT in 35 MPa of gaseous hydrogen. As shown in Fig.1, this facility consists in a high-pressure autoclave assembled to a servo-hydraulic testing machine, with a maximum operation pressure and temperature of 40 MPa and 150ºC, respectively. For more details see [19].

Fig. 1. Hycomat test bench used to perform in-situ FCGR tests.

In order to meet the dimensional requirements of the facility, the CT specimens had a width of 40 mm, a thickness of 10 mm and an initial crack length, $a_0$=7 mm (a/W=0.17). The specimens were fatigue pre-cracked in air (R=0.1 and 10 Hz).

The tests were performed under loading control from $\Delta K_0$=30 MPa$\sqrt{m}$ at R=0.1 under f=1 and 0.1 Hz, in order to compare the results with those obtained on pre-charged specimens. Crack length was measured by optical microscope and DCPD during the tests. The initial and final crack lengths were measured on the fracture surface of the broken specimen, and the measured ΔK values were corrected.

### *2.3. Fracture surface observation*

After the completion of the FCGRT, the CT specimens were carefully cut and rinsed with acetone. In order to identify the operative fracture micromechanisms, the fracture surfaces of all the tested specimens were observed under different magnifications in a scanning electron microscope SEM JEOL-JSM5600 under 20 kV.

## 3. Results

### *3.1. Hydrogen pre-charged specimens*

The da/dN vs. ΔK curves for uncharged and hydrogen pre-charged CT specimens corresponding to the BS and the CGHAZ are shown in Fig. 2. In general, the presence of internal hydrogen induces an important increase in the FCGR on both the BS and the CGHAZ when tested at 0.1 Hz.

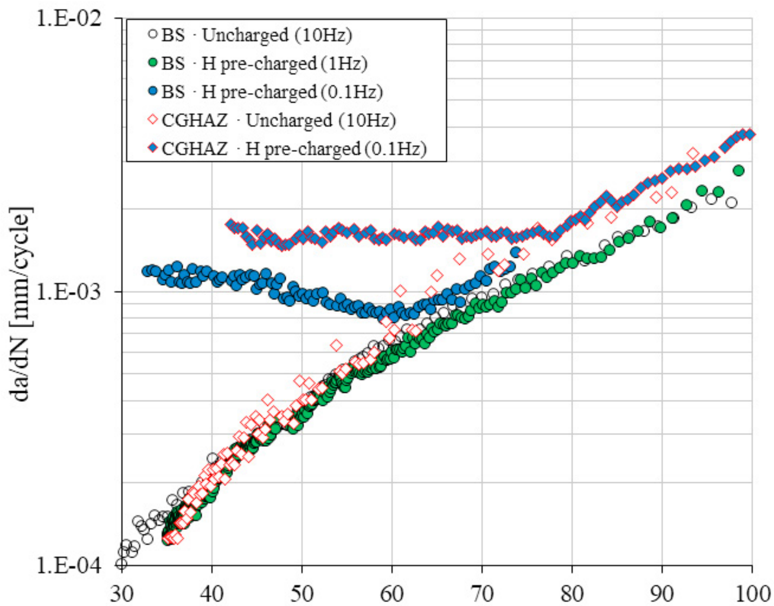


Fig. 2. da/dN vs. ΔK curves of the BS and CGHAZ in uncharged and hydrogen pre-charged conditions. R=0.1.

Comparing first the curves of uncharged specimens, the CGHAZ shows a similar behavior than the BS, and striation marks indicative of ductile cyclic failure are detected in both cases, as shown in Fig. 3. However, from ΔK values larger than 60 MPa$\sqrt{m}$, the FCGR of the CGHAZ becomes slightly higher than the BS (about 1.5 times), and although striation marks are still visible in the fracture surface, the overall fracture micromechanism becomes more brittle. This behavior was previously observed by Vargas-Arista et al. [20] in the HAZ of a 42CrMo4 steel with similar yield strength.

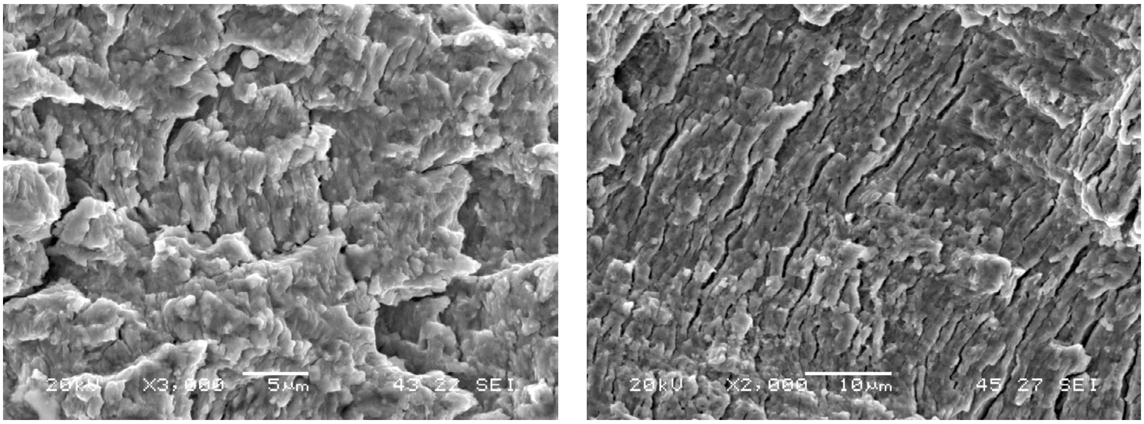


(a) (b)

Fig. 3. Fracture surface at $\Delta K=35MPa\sqrt{m}$ of hydrogen uncharged specimens (R=0.1 and f=10 Hz). (a) BS and (b) CGHAZ.

When the base steel specimens are tested with internal hydrogen at 1 Hz the curve overlaps that of the uncharged specimens. Striation marks were still characteristic of their fracture surface, so that hydrogen does not modify the fatigue behavior at this frequency. However, at a frequency 10 times lower, 0.1 Hz, the hydrogen effects became remarkable at intermediate ΔK values, being the FCGR around 7 times greater than in uncharged specimens. The characteristic striation marks are not observed in the BS specimens tested with internal hydrogen at 0.1 Hz, being now the fracture surface characterized by martensitic lath decohesion (MLD), as shown in Fig. 4. This failure micromechanism is associated to the decrease of the cohesive strength among lath martensite interfaces promoted by hydrogen. Other authors [21,22] have already pointed out the disappearance of fatigue striations in fatigue tests performed in the presence of hydrogen.

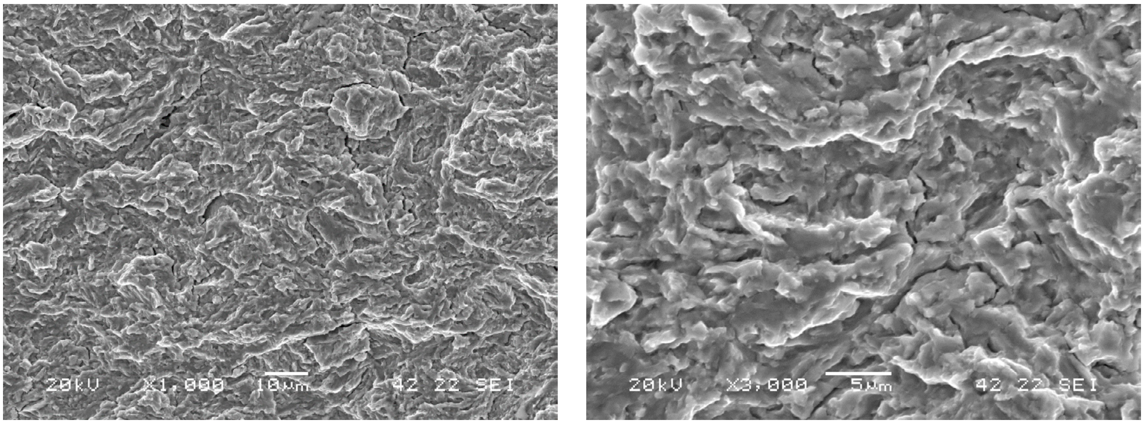


(a) (b)

Fig. 4. Fracture surface at $\Delta K=35MPa\sqrt{m}$ of hydrogen pre-charged specimens of the BS tested at R=0.1 and f=0.1 Hz. (a) 1000x and (b) 3000x.

In the case of the CGHAZ tested at 0.1 Hz hydrogen gives rise to an acceleration of the FCGR even higher than in the BS, about two times greater. This worst fatigue behaviour is also manifested in a drastic change in the operative fracture micromechanism, as can be observed in Fig. 5. Indeed, the fatigue fracture surfaces of the CGHAZ are characterized by the combination of intergranular (IG) and MLD. It is worth noting the large size of the prior austenitic grains of the CGHAZ.

In general, it is remarkable the influence of the testing frequency on the acceleration of the FCGR: the maximum hydrogen effects are displayed at a low testing frequency of 0.1 Hz. It is also interesting to mention that under this low frequency, da/dN remains practically constant from the beginning of the test ($\Delta K \approx 30\text{-}35MPa\sqrt{m}$) up to a ΔK value of approximately 60-70 MPa$\sqrt{m}$, when the curve converge with that of the uncharged specimens. This "plateau" region, already observed by other authors [18], will be discussed later. Anyway, the FCGR of hydrogen pre-charged specimens was always greater in the CGHAZ than in the BS, and more brittle operative micromechanisms were also observed.

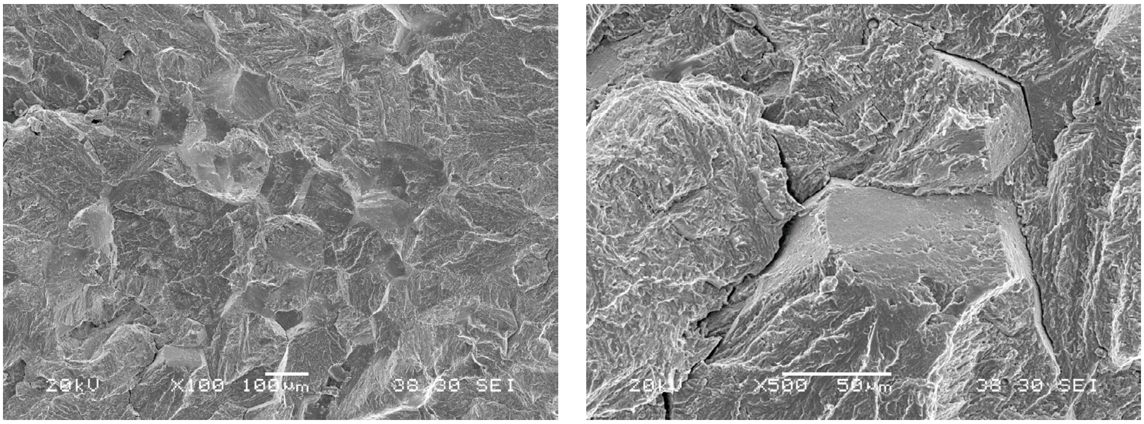


Fig. 5. Fracture surface at ΔK=45MPa$\sqrt{m}$ of hydrogen pre-charged specimens of the CGHAZ tested at R=0.1 and f=0.1 Hz.

### 3.2. Specimens tested in 35 MPa hydrogen

Fig. 6 shows the da/dN vs. ΔK curves of BS and CGHAZ specimens tested in air (uncharged) and in 35 MPa of pure hydrogen.

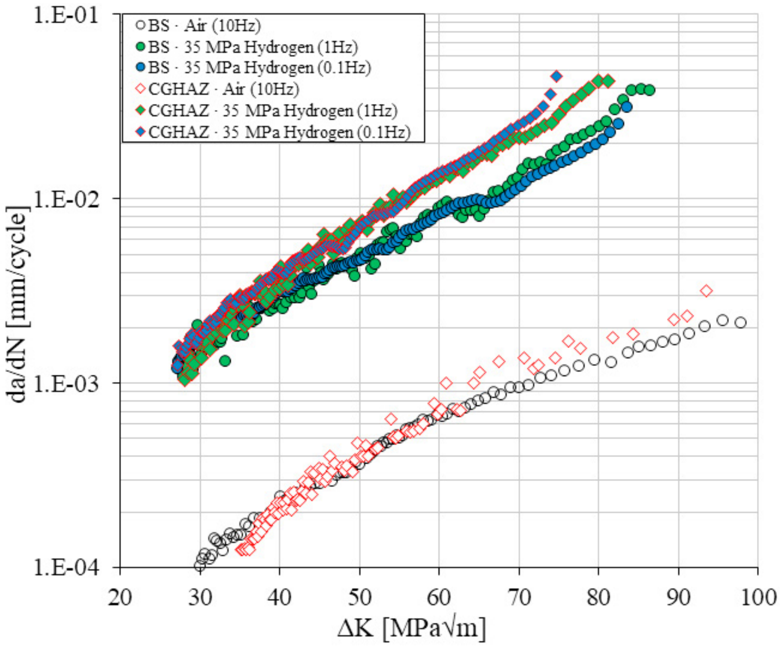


Fig. 6. da/dN vs. ΔK curves of the BS and CGHAZ tested in air and in 35 MPa of pure hydrogen. R=0.1.

A great acceleration of the FCGR due to hydrogen in all the ΔK spectrum at both tested frequencies (1 Hz and 0.1 Hz) is worth noting. In this case, there is no influence of the test frequency, which is in line with the observations made by other authors [8]. For example, Stewart [23] did not report any difference in the FCGR curves in a 2NiCrMoV steel tested in 40 MPa of pure hydrogen between frequencies of 1 and 0.01 Hz.

On the other hand, the difference between the fatigue crack growth rate curves of the BS and the CGHAZ measured under 35 MPa of hydrogen continuously increases until the end of the tests. Figs. 7 and 8 show the fracture surfaces of both BS and CGHAZ tested in 35 MPa of hydrogen at 0.1 Hz. The operative mechanism in the BS was MLD and in the CGHAZ a combination of IG and MLD. It is also worth to mention that no significant differences in the fracture micromechanisms were observed at different crack lengths (different ΔK) in any of the steels, as can be appreciated for example comparing Fig. 8(a) and (b).

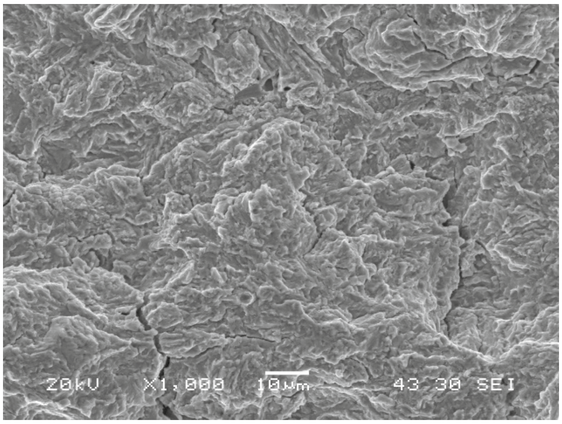


Fig. 7. Fracture surface at ΔK=40MPa$\sqrt{m}$ of BS specimens tested in 35MPa hydrogen gas at R=0.1 and f=0.1 Hz.

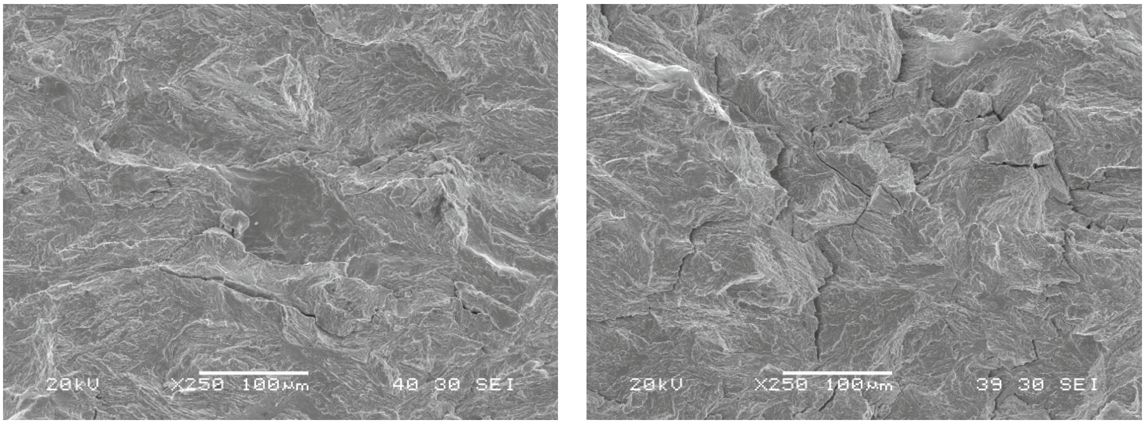


(a) (b)

Fig. 8. Fracture surface of BS specimens tested in 35MPa hydrogen gas at R=0.1 and f=0.1 Hz at (a) at ΔK=30MPa$\sqrt{m}$ and (b) ΔK=60MPa$\sqrt{m}$

## 4. Discussion

The discussion of this paper is focused on the comparison of the two testing methodologies employed in this work to assess the influence of hydrogen on the crack growth rate of a 42CrMo4 steel weld. Therefore, Fig. 9 presents the da/dN-ΔK curves of the BM and the CGHAZ tested at R=0.1 and f=0.1 Hz obtained with pre-charged and in-situ hydrogen conditions.

A "plateau" region characterized by a constant da/dN crack growth rate is observed in the pre-charged samples, while a typical growing linear trend (Paris propagation region) is characteristic in the specimens tested in 35 MPa hydrogen. The da/dN acceleration factor (da/dN measured in the presence of hydrogen over da/dN measured in non-charged specimens tested in air), Table 2, is much greater in the in-situ tested specimens and is practically constant along all the ΔK range. These results are justified assuming hydrogen accumulation in the process zone is quite different under both testing conditions.

Hydrogen concentrations between 1.2 and 1 wppm were measured in both steels after extraction from the hydrogen reactor (pre-charged specimens). The plateau observed with the pre-charged specimens may be explained by: (I) hydrogen losses that take place in the course of the test and (II) hydrogen re-distribution in the process region (plastic zone) located ahead of the crack tip. Both reasons would result in a progressive reduction of the hydrogen concentration in the process zone during crack growth (larger ΔK).

On the contrary, hydrogen is continuously provided to the process zone when the specimen is kept at a high hydrogen pressure during all the test. In this case, hydrogen absorption takes place in the crack front where plastic deformation attains very large values, being well known that hydrogen saturation largely increases with the applied plastic deformation [24,25].

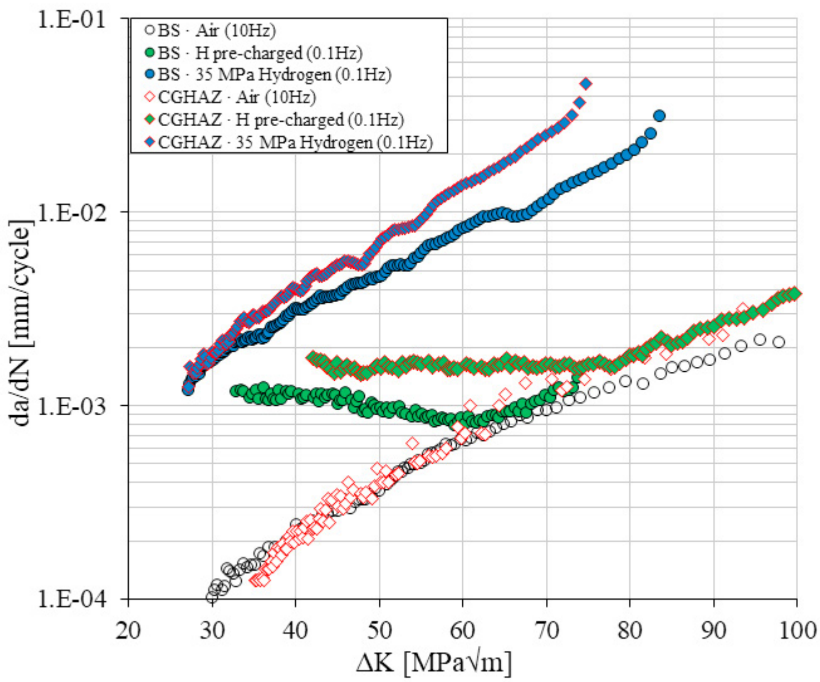


Fig. 9. da/dN vs. ΔK curves of the BS and CGHAZ tested in air and in 35 MPa pure hydrogen. R=0.1.

Table 2. Acceleration of the FCGR due to hydrogen in the BS and the CGHAZ. (da/dN)H/(da/dN)air

| Testing methodology | Steel | ΔK [MPa$\sqrt{m}$] | | | | | | | |
|---|---|---|---|---|---|---|---|---|---|
| | | 35 | 40 | 45 | 50 | 55 | 60 | 65 | 70 |
| Pre-charge | BM | 7.6 | 5.0 | 3.4 | 2.6 | 1.8 | 1.3 | 1.2 | 1.2 |
| (1.2-1.0 wppm H) | CGHAZ | - | 14.1 | 7.0 | 5.0 | 3.8 | 3.0 | 2.4 | 1.4 |
| In-situ | BM | 14.7 | 13.0 | 13.0 | 12.7 | 12.2 | 12.6 | 12.1 | 12.4 |
| (35 MPa $H_2$) | CGHAZ | 23.6 | 18.0 | 17.7 | 17.3 | 16.8 | 19.7 | 15.8 | 19.1 |

This also explains that the behavior of pre-charged specimens is greatly affected by the testing frequency, as pre-charged hydrogen needs a certain time to diffuse from the surroundings until attaining the accumulation needed to embrittle the process zone. On the contrary, hydrogen diffusion distances from the crack tip to the process zone are very small in the in-situ tests and the existence of very high local plastic deformation in this region also enhances hydrogen diffusion (hydrogen transported by dislocations) [26], providing high accumulation of hydrogen even under quite large testing frequencies (1 Hz).

An interesting fact to highlight is that despite the great difference observed in the FCGR behavior when using both testing methodologies, the modification of the fracture micromechanisms due to hydrogen was practically the same in both cases. Hydrogen failure micromechanisms (martensite lath decohesion and intergranular fracture) occur when a critical accumulation of hydrogen is attained in the process zone and as this local hydrogen concentration increases (in-situ tests), failure micromechanisms are not modified but extended to embrittle larger regions (increasing the fatigue crack growth per cycle). In addition, the CGHAZ showed a considerable worst fatigue performance in presence of hydrogen than the BS, intergranular failure micromechanism develops also in the latter case and this was observed under both testing conditions, with pre-charged samples and under in-situ testing.

However, in light of the results shown in Table 2, even at low ΔK values, where the hydrogen effects on the FCGR in hydrogen pre-charged specimens are important, tests performed on hydrogen pre-charged specimens do not represent the actual performance of ferritic steels in contact with high-pressure hydrogen atmosphere, where FCGR are significantly larger.

## 5. Conclusions

FCGR determined by means of in-situ tests performed under high-pressure hydrogen (35MPa) is much larger than the corresponding values obtained using pre-charged specimens. In the former case, hydrogen is continuously provided to the process zone during all the test. Hydrogen absorption takes place in the crack front where plastic deformation attains very large values, giving rise to higher and more extended hydrogen accumulations.

The fatigue behavior of the pre-charged specimens is largely affected by the testing frequency, but it is not affected in the case of the in-situ tests. Even when performed at the same frequencies, the diffusion distances needed to reach the process zone and in turn the amount of hydrogen accumulated in this region are very different in both type of tests.

The presence of hydrogen modifies the fatigue failure micromechanism observed in the steels, taking place martensite lath decohesion and intergranular fracture (only in the CGHAZ) under both type of hydrogen testing conditions, pre-charged specimens and in-situ tests.

## Acknowledgements

The authors would like to thank the Spanish Ministry of Science, Innovation and Universities for the financial support received to carry out research project RTI2018-096070-B-C31 (H2steelweld), and A. Zafra and G. Álvarez to the Ministry of Education and Culture of the Principality of Asturias for the Severo Ochoa grants PA-18-PF-BP17-038 and PA-20-PF-BP19-087, respectively. Finally, the authors would also like to acknowledge the technical support provided by the Scientific and Technical Service of the University of Oviedo for the use of the SEM JEOLJSM5600 scanning electron microscope.

## References

[1] S.E. Hosseini, M.A. Wahid, Hydrogen production from renewable and sustainable energy resources: Promising green energy carrier for clean development, Renew. Sustain. Energy Rev. 57 (2016) 850–866. https://doi.org/10.1016/j.rser.2015.12.112.

[2] Y. Ogawa, H. Matsunaga, J. Yamabe, M. Yoshikawa, S. Matsuoka, Unified evaluation of hydrogen-induced crack growth in fatigue tests and fracture toughness tests of a carbon steel, Int. J. Fatigue. 103 (2017) 223–233. https://doi.org/10.1016/j.ijfatigue.2017.06.006.

[3] M. Nagumo, Fundamentals of hydrogen embrittlement, 2016. https://doi.org/10.1007/978-981-10-0161-1.

[4] Q. Liu, A. Atrens, A critical review of the influence of hydrogen on the mechanical properties of medium-strength steels, Corros. Rev. 31 (2013) 85–103. https://doi.org/10.1515/corrrev-2013-0023.

[5] L. Tau, S.L.I. Chan, C.S. Shin, Hydrogen enhanced fatigue crack propagation of bainitic and tempered martensitic steels, Corros. Sci. 38 (1996) 2049–2060. https://doi.org/10.1016/S0010-938X(96)89123-2.

[6] Y. Murakami, R.O. Ritchie, Effects of hydrogen on fatigue-crack propagation in steels, Gaseous Hydrog. Embrittlement Mater. Energy Technol. Probl. Its Characterisation Eff. Part. Alloy Classes. (2012) 379–417. https://doi.org/10.1533/9780857093899.2.379.

[7] A. Alvaro, D. Wan, V. Olden, A. Barnoush, Hydrogen enhanced fatigue crack growth rates in a ferritic Fe-3 wt%Si alloy and a X70 pipeline steel, Eng. Fract. Mech. 219 (2019) 106641. https://doi.org/10.1016/j.engfracmech.2019.106641.

[8] K.A. Nibur, B.P. Somerday, Fracture and fatigue test methods in hydrogen gas, Gaseous Hydrog. Embrittlement Mater. Energy Technol. Probl. Its Characterisation Eff. Part. Alloy Classes. (2012) 195–236. https://doi.org/10.1533/9780857093899.2.195.

[9] R.P. Gangloff, B.P. Somerday, Gaseous Hydrogen Embrittlement of Materials in Energy Technologies: Mechanisms, Modelling and Future Developments, Woodhead Publishing, 2012. https://doi.org/10.1533/9780857095374.

[10] L. Briottet, I. Moro, M. Escot, J. Furtado, P. Bortot, G.M. Tamponi, J. Solin, G. Odemer, C. Blanc, E. Andrieu, Fatigue crack initiation and growth in a CrMo steel under hydrogen pressure, Int. J. Hydrogen Energy. 40 (2015) 17021–17030. https://doi.org/10.1016/j.ijhydene.2015.05.080.

[11] K. Tazoe, S. Hamada, H. Noguchi, Fatigue crack growth behavior of JIS SCM440 steel near fatigue threshold in 9-MPa hydrogen gas environment, Int. J. Hydrogen Energy. 42 (2017) 13158–13170. https://doi.org/10.1016/j.ijhydene.2017.03.223.

[12] A. Macadre, M. Artamonov, S. Matsuoka, J. Furtado, Effects of hydrogen pressure and test frequency on fatigue crack growth properties of Ni–Cr–Mo steel candidate for a storage cylinder of a 70MPa hydrogen filling station, Eng. Fract. Mech. 78 (2011) 3196–3211. https://doi.org/10.1016/j.engfracmech.2011.09.007.

[13] J. Yamabe, H. Matsunaga, Y. Furuya, S. Hamada, H. Itoga, M. Yoshikawa, E. Takeuchi, S. Matsuoka, Qualification of chromium-molybdenum steel based on the safety factor multiplier method in CHMC1-2014, Int. J. Hydrogen Energy. 40 (2015) 719–728. https://doi.org/10.1016/j.ijhydene.2014.10.114.

[14] L.B. Peral, A. Zafra, S. Blasón, C. Rodríguez, J. Belzunce, Effect of hydrogen on the fatigue crack growth rate of quenched and tempered CrMo and CrMoV steels, Int. J. Fatigue. 120 (2019) 201–214. https://doi.org/10.1016/j.ijfatigue.2018.11.015.

[15] S.A. Ahmad, D.A. Ryder, T.J. Davies, On the embrittlement of fracture toughness specimens of two high strength steels, Eng. Fract. Mech. 7 (1975) 357–365.

[16] L.W. Tsay, C.C. Liu, Y.H. Chao, Y.H. Shieh, Fatigue crack propagation in 2.25 Cr-1.0Mo steel weldments in air and hydrogen, Mater. Sci. Eng. A. 299 (2001) 16–26. https://doi.org/10.1016/S0921-5093(00)01420-9.

[17] A. Zafra, F.J. Belzunce, C. Rodríguez, I. Fernández-Pariente, Hydrogen embrittlement of the coarse grain heat affected zone of a quenched and tempered 42CrMo4 steel, Int. J. Hydrogen Energy. (2020).

[18] C. Colombo, G. Fumagalli, F. Bolzoni, G. Gobbi, L. Vergani, Fatigue behavior of hydrogen pre-charged low alloy Cr-Mo steel, Int. J. Fatigue. 83 (2015) 2–9. https://doi.org/10.1016/j.ijfatigue.2015.06.002.

[19] Z. Sun, C. Moriconi, G. Benoit, D. Halm, G. Henaff, Fatigue crack growth under high pressure of gaseous hydrogen in a 15-5PH martensitic stainless steel: Influence of pressure and loading frequency, Metall. Mater. Trans. A Phys. Metall. Mater. Sci. 44 (2013) 1320–1330. https://doi.org/10.1007/s11661-012-1133-5.

[20] B. Vargas-Arista, J. Teran-Guillen, J. Solis, G. Garcia-Cerecero, M. Martinez-Madrid, Normalizing effect on fatigue crack propagation at the heat-affected zone of AISI 4140 steel shielded metal arc weldings, Mater. Res. 16 (2013) 772–778. https://doi.org/10.1590/S1516-14392013005000047.

[21] Y. Murakami, S. Matsuoka, Effect of hydrogen on fatigue crack growth of metals, Eng. Fract. Mech. 77 (2010) 1926–1940. https://doi.org/10.1016/j.engfracmech.2010.04.012.

[22] S. Matsuoka, H. Tanaka, N. Homma, Y. Murakami, Influence of hydrogen and frequency on fatigue crack growth behavior of Cr-Mo steel, Int. J. Fract. 168 (2011) 101–112. https://doi.org/10.1007/s10704-010-9560-z.

[23] Stewart A.T., The effect of hydrogen on fatigue crack propagation in steels, in: Mech. Environ. Sensitive Crack. Mater., The Metals Society, 1977: pp. 400–410.

[24] A. Zafra, J. Belzunce, C. Rodríguez, Hydrogen diffusion and trapping in 42CrMo4 quenched and tempered steel: influence of quenching temperature and plastic deformation, Mater. Chem. Phys. 255 (2020) 123599.

[25] A. Zafra, Study on hydrogen diffusivity and embrittlement of quenched and tempered 42CrMo4 steel, PhD Thesis, University of Oviedo, Spain, 2021.

[26] M.L. Martin, M. Dadfarnia, A. Nagao, S. Wang, P. Sofronis, Enumeration of the hydrogen-enhanced localized plasticity mechanism for hydrogen embrittlement in structural materials, Acta Mater. 165 (2019) 734–750. https://doi.org/10.1016/j.actamat.2018.12.014.